

Profound change of the near-Earth radiation environment caused by solar superstorms

Y. Y. Shprits^{1,2,3},

R. Horne⁴, D. Subbotin³ , B. Ni³, D. Baker⁴

¹ IGPP, UCLA, CA, Los Angeles, USA, yshprits@atmos.ucla.edu

² ESS, UCLA, Los Angeles, CA, USA

³ AOS, UCLA, Los Angeles, CA, USA

⁴ BAS, Cambridge, UK

⁵ LASP, Boulder, CO , USA, 90095

Space weather and it's effects

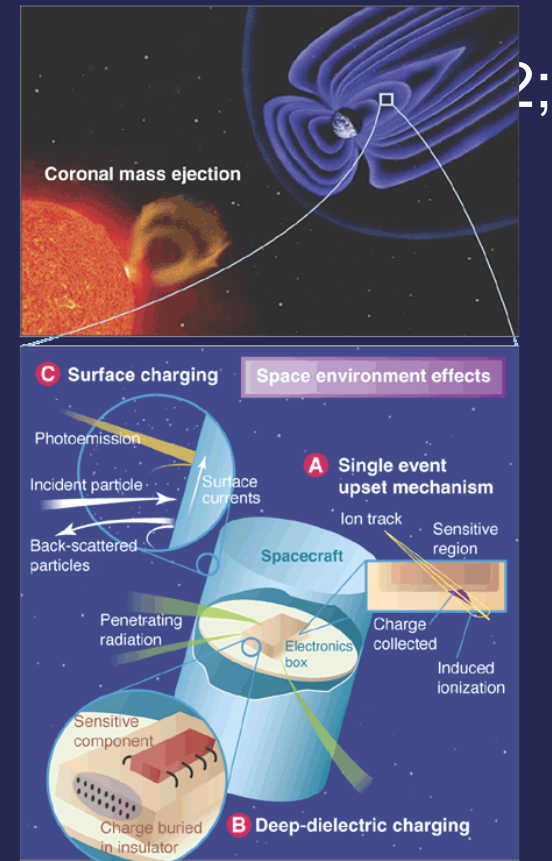
~250 satellites; Supporting \$25 billion/year industry ;Replacement cost: \$75 billion;

Space weather–induced effects on an Earth-orbiting spacecraft:

(A) Single-event upsets (SEUs) due to energetic ions;

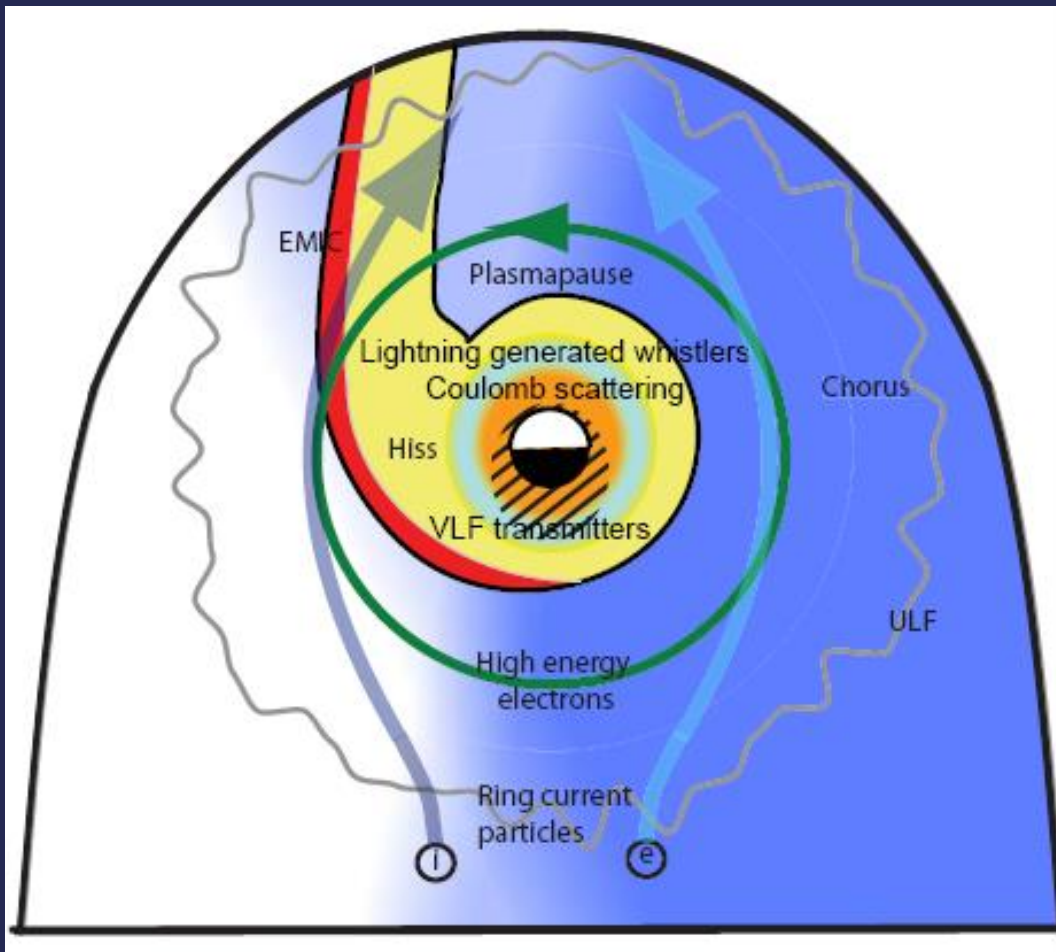
(B) Deep-dielectric charging due to relativistic electrons;

(C) Surface charging due to moderate-energy electrons.



[Baker et al., 2006]

Competition between acceleration and loss during storm time



Inward radial diffusion driven by ULF magnetic field.

Energy and Pitch angle scattering due to resonance interactions with different waves

Combined effect of losses to magnetopause and outward radial diffusion.

[Shprits et al., 2008; Review JASTP]

Fokker-Planck Equation

$$\begin{aligned} \frac{\partial f}{\partial t} = & L^{*2} \frac{\partial}{\partial L^*} \bigg|_{J_1, J_2} \frac{1}{L^{*2}} D_{L^* L^*} \frac{\partial f}{\partial L^*} \bigg|_{J_1, J_2} + \\ & + \frac{1}{p^2} \frac{\partial}{\partial p} \bigg|_{L, \alpha_0} p^2 \left(D_{pp} \frac{\partial f}{\partial p} \bigg|_{L, \alpha_0} + D_{p\alpha_0} \frac{\partial f}{\partial \alpha_0} \bigg|_{L, p} \right) + \\ & + \frac{1}{T(\alpha_0) \sin(2\alpha_0)} \frac{\partial}{\partial \alpha_0} \bigg|_{L, p} T(\alpha_0) \sin(2\alpha_0) \left(D_{\alpha_0 p} \frac{\partial f}{\partial p} \bigg|_{L, \alpha_0} + D_{\alpha_0 \alpha_0} \frac{\partial f}{\partial \alpha_0} \bigg|_{L, p} \right) + \\ & - \frac{f}{\tau_{loss\ cone}} - \frac{f}{\tau_{coulomb}} \end{aligned}$$

Outer boundary is set up at L=5.5 .

Parametrizations are driven by the Kp index.

FP equation accounts for the radial, mixed , and energy diffusion

$$\begin{aligned} \tau_{losscone}(\text{sec}) &= 1/4 \tau_b & \tau_{coulomb}(\text{sec}) &= 3 \times 10^8 E[\text{keV}]^{3/2} / N(L^*) \\ \text{where } \tau_b &\text{ is the electron bounce time} & \text{where } N(L^*) &= 1000(4/L^*)^4 \text{ in units of cm}^{-3} \end{aligned}$$

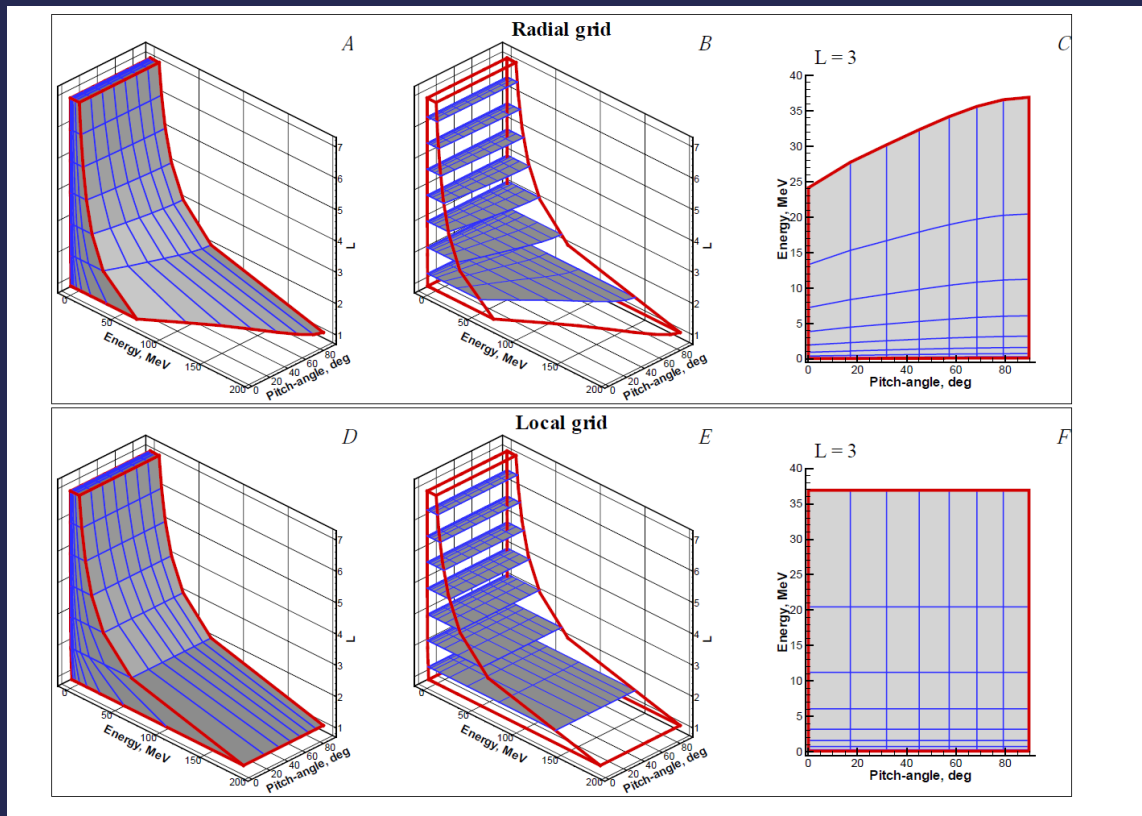
Inward **radial diffusion** can redistribute fluxes and provide energization or loss

Pitch angle scattering produces loss of electrons to the atmosphere

Energy diffusion provides local source of particles

[e.g. Schulz and Lanzerotti, 1974; Schulz, 1991; Shprits et al., 2009]

VERB Code Simulation Grids

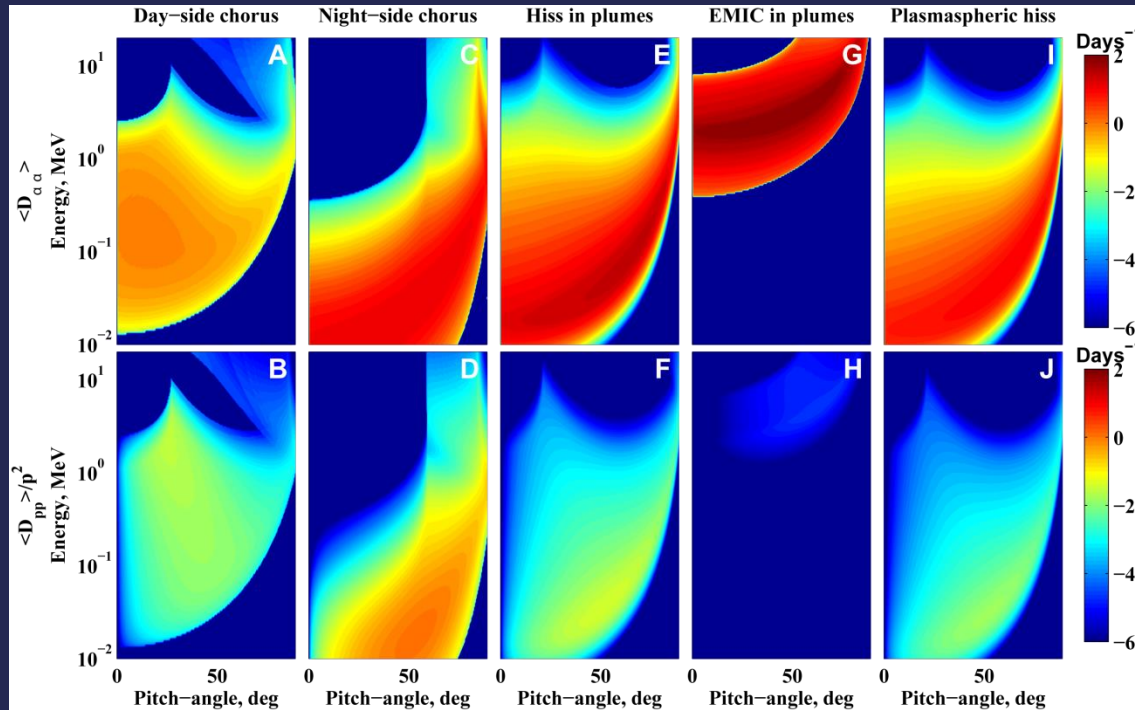


[Subbotin and Shprits, 2009]

VERB code uses two grids. One is used to compute radial diffusion *radial grid*, and *local grid* is used for computations of pitch-angle, energy, and mixed diffusion.

We use the spline interpolaiton to map phase space density between local and radial grids.

Pitch-angle and energy diffusion coefficients due to resonant wave-particle interactions

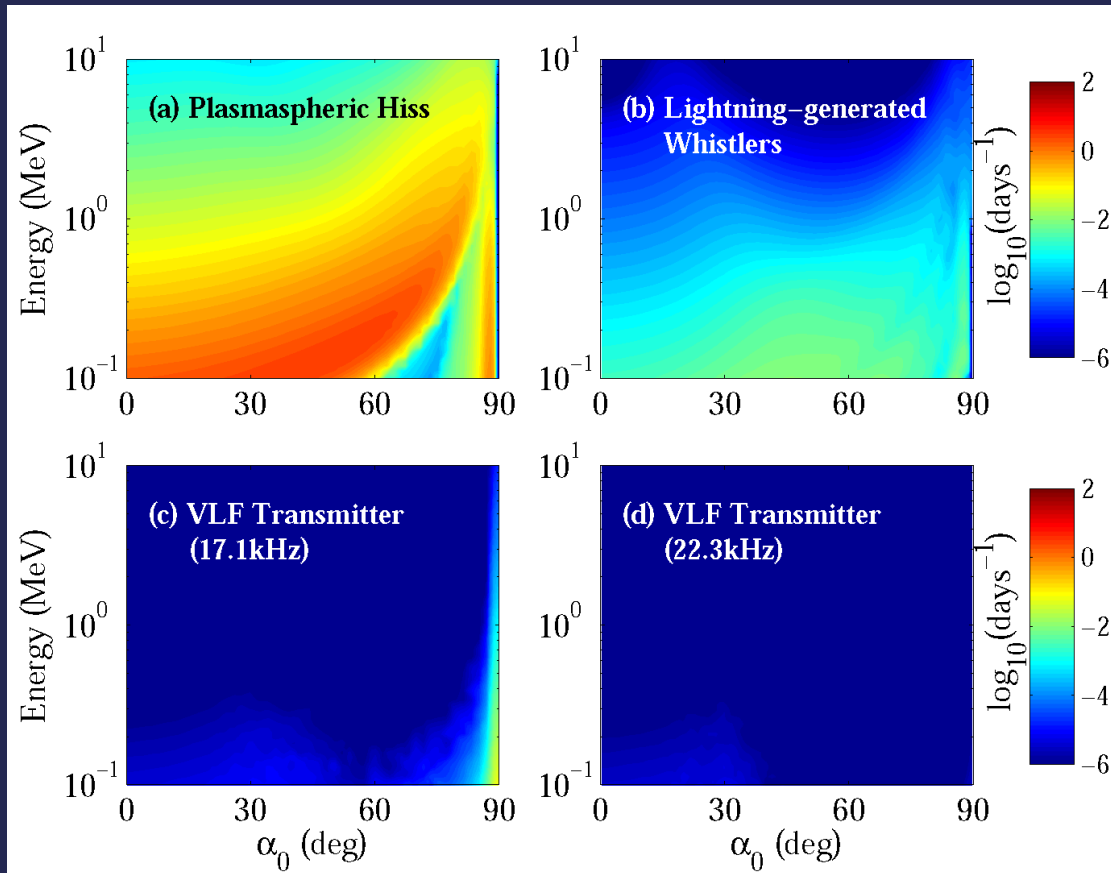


Pitch-angle diffusion results in a loss to the atmosphere

Energy diffusion can accelerate electrons locally

Diffusion rates as due to resonance wave particle interactions with various plasma waves.

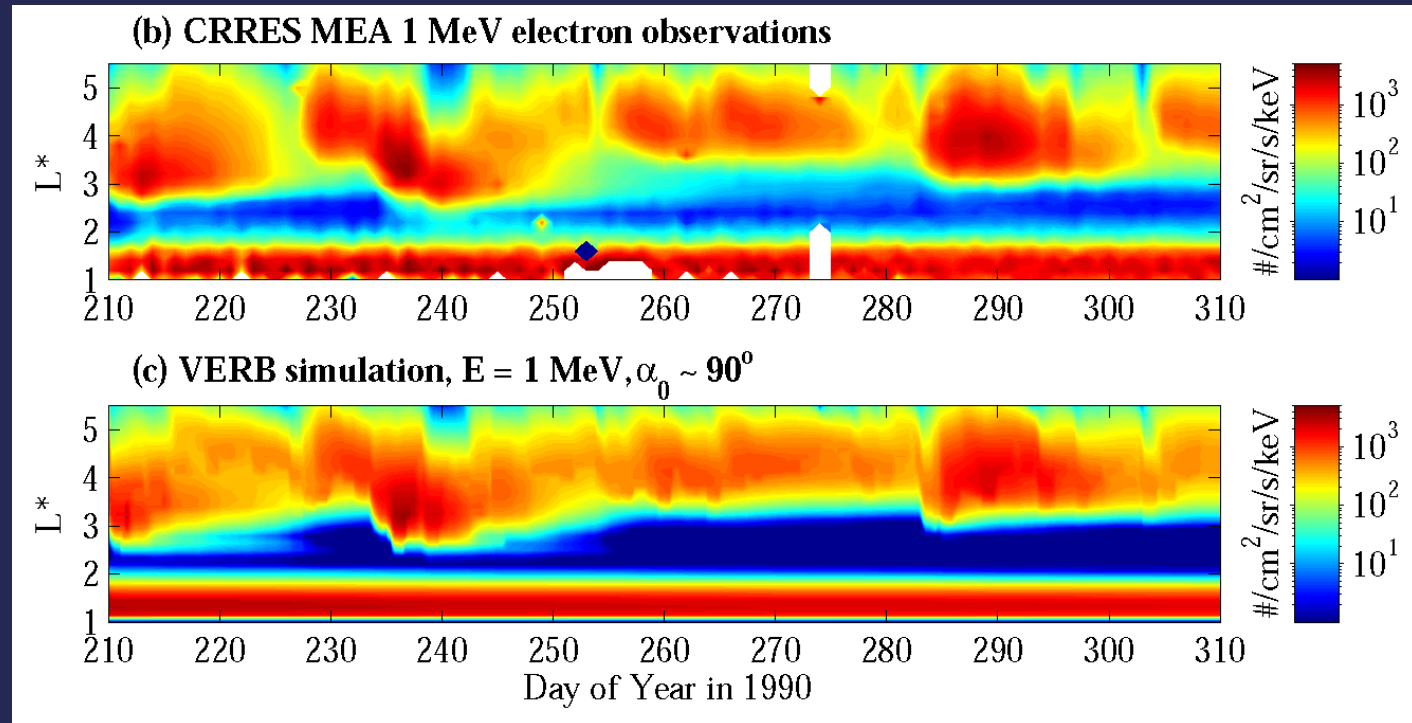
Bounce-averaged pitch angle diffusion coefficients calculated at $L^* = 3$



Pitch-angle scattering rates for the plasmaspheric hiss are significantly higher than those for the other types of waves. Since the anthropogenic VLF were corrected according to Starks et al. [2008], their effect becomes negligible.

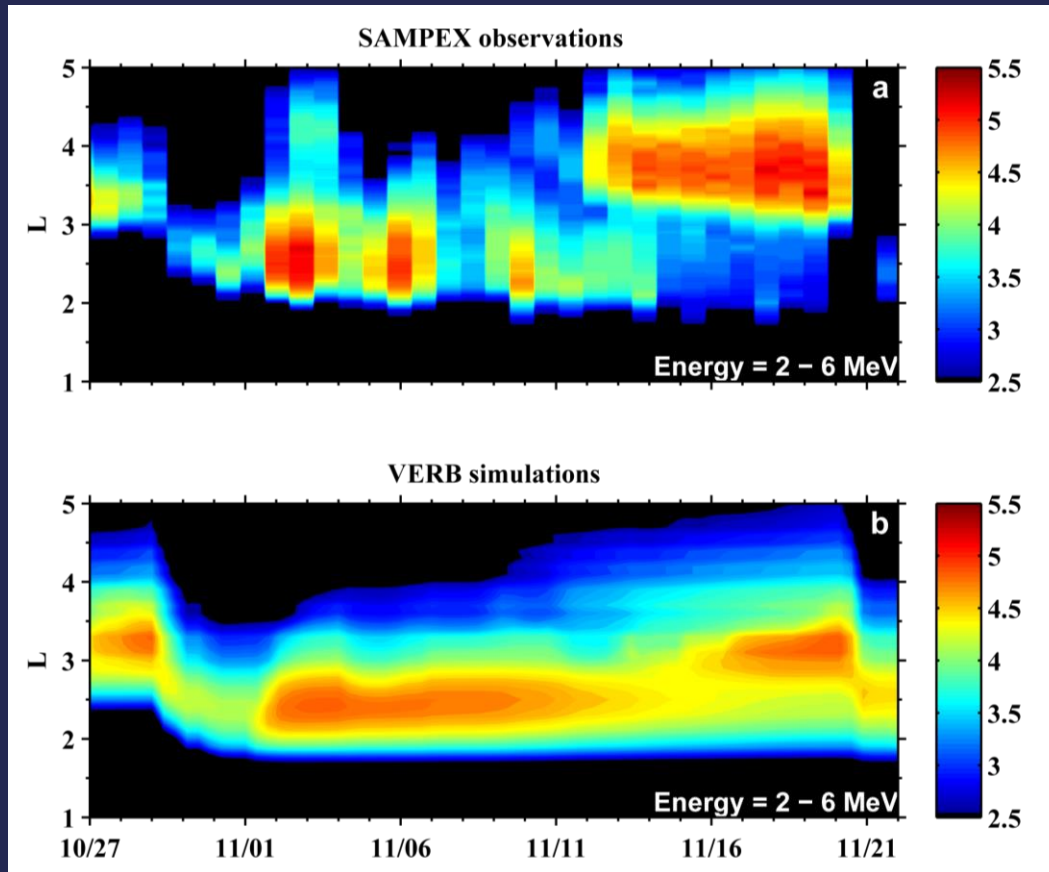
[Kim et al, 2011]

Validation of the VERB code over 100 days in 1990



- VERB predicts the instantaneous location of the upper boundary of the slot region, the empty slot region, the stable inner belts, the location of peak of fluxes and amplitude of fluxes.

Observations (a) and Modeling (b) of the Halloween Storms in 2003

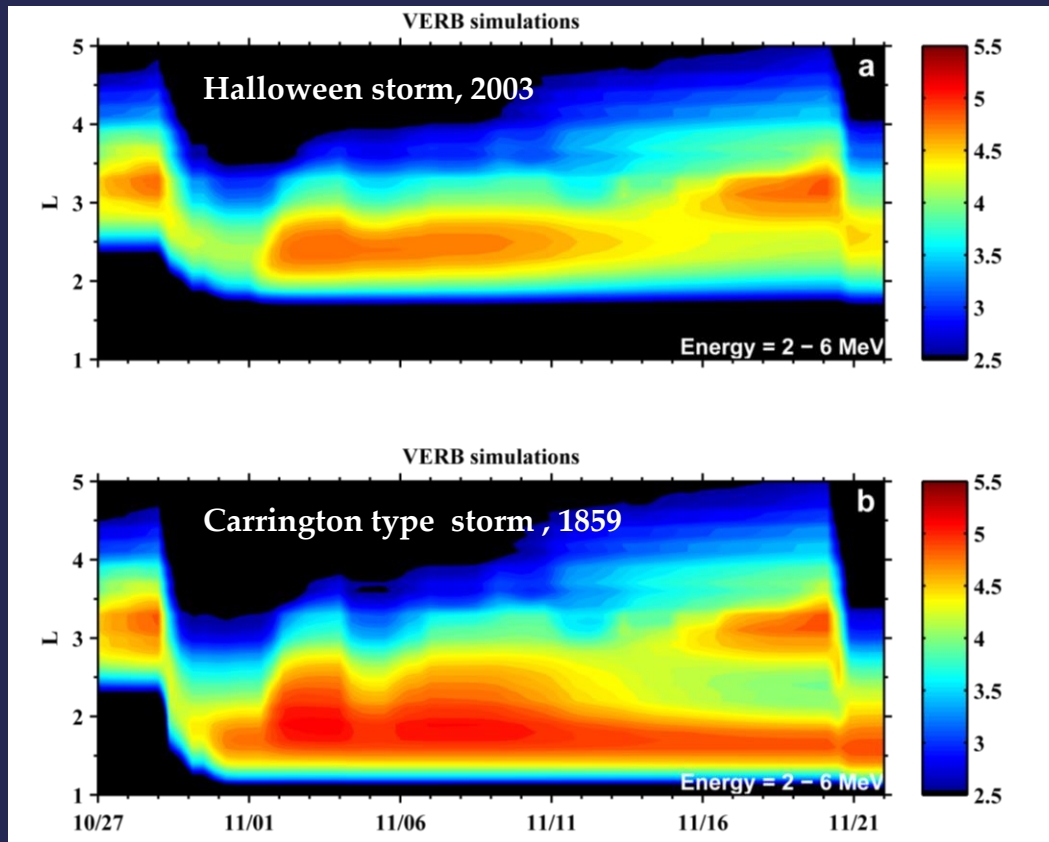


VERB code which now includes radial transport, pitch-angle scattering, and mixed diffusion scattering can reproduce the observed unusual dynamics of fluxes during this storm.

Only Kp index is used as the input for the simulations.

[Shprits et al., 2011]

Simulations of the 2003 Halloween storm and 1859 Carrington superstorm

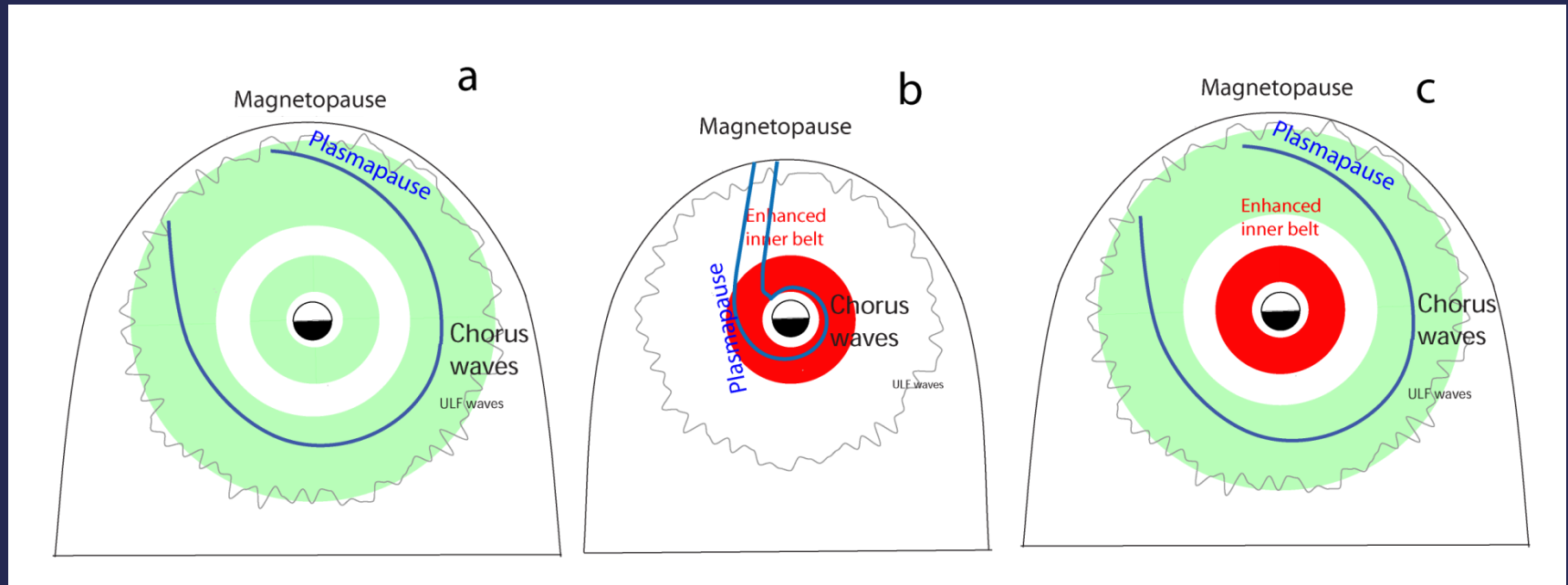


(a) VERB code simulations of the dynamics of the radiation belts for the 2003 Halloween storm.

(b) VERB code simulations of the dynamics of the radiation belts during a superstorm similar to Carrington storm in 1859

[Shprits et al, 2011]

Dynamics of the Radiation Belts During Solar Superstorms



Acceleration in the inner belt enhances inner radiation belt fluxes. Enhanced fluxes will persist for up to a decade.

[Shprits et al, 2011]

Summary I

- Dynamics of the radiation belts is driven by **the radial, pitch-angle, energy, and mixed diffusion** due to various ULF, VLF, and ELF waves.
- Both radial diffusion and energy diffusion are responsible for acceleration of electrons to relativistic energies.
- Modeling with VERB code which now includes radial, pitch-angle, energy, and mixed diffusion can reproduce the general dynamics of the CME and CIR driven storms.
- VERB model can capture the dynamics of the relativistic electron fluxes during **long term simulations** as well as observations of the unusual behavior of the radiation belts during **Halloween storms**.

Summary II

- Modeling of the Carrington type superstorm shows that electrons may be accelerated to MeV energies inside the inner zone, where they **will persist several years**.
- GEANT 4 simulations show that such intensification will increase the dose on a typical spacecraft traversing the inner zone by a factor of 10.
- Such intensification in the inner zone may significantly **decrease the lifetime** of spacecraft operating in the **inner zone**.
- Future work should include estimation of risks, probabilities of such events and climatological estimates of the location of the plasmopause and parameters of waves during strong storms